Draft version September 21, 2009
Preprint typeset using LaTeX style emulateapj v. 08/22/09

THE PHYSICAL ORIGIN AND THE DIAGNOSTIC POTENTIAL OF THE SCATTERING POLARIZATION IN THE LITHIUM RESONANCE DOUBLET AT 6708 Å

Luca Belluzzi[1], Egidio Landi Degl'Innocenti[2,1] and Javier Trujillo Bueno[2,3]
[1]Dipartimento di Astronomia e Scienza dello Spazio, Università di Firenze, Largo E. Fermi 2, I-50125 Firenze, Italy
[2]Instituto de Astrofísica de Canarias, Vía Láctea s/n, E-38205 La Laguna, Tenerife, Spain
[3]Consejo Superior de Investigaciones Científicas, Spain
Draft version September 21, 2009

ABSTRACT

High-sensitivity measurements of the linearly-polarized solar limb spectrum produced by scattering processes in quiet regions of the solar atmosphere showed that the Q/I profile of the lithium doublet at 6708 Å has an amplitude $\sim 10^{-4}$ and a curious three-peak structure, qualitatively similar to that found and confirmed by many observers in the Na I D_2 line. Given that a precise measurement of the scattering polarization profile of the lithium doublet lies at the limit of the present observational possibilities, it is worthwhile to clarify the physical origin of the observed polarization, its diagnostic potential and what kind of Q/I shapes can be expected from theory. To this end, we have applied the quantum theory of atomic level polarization taking into account the hyperfine structure of the two stable isotopes of lithium, as well as the Hanle effect of a microturbulent magnetic field of arbitrary strength. We find that quantum interferences between the sublevels pertaining to the upper levels of the D_2 and D_1 line transitions of lithium do not cause any observable effect on the emergent Q/I profile. Our theoretical calculations show that only two Q/I peaks can be expected, with the strongest one caused by the D_2 line of ^{7}Li I and the weakest one due to the D_2 line of ^{6}Li I. Interestingly, we find that these two peaks in the theoretical Q/I profile stand out clearly only when the kinetic temperature of the thin atmospheric region that produces the emergent spectral line radiation is lower than 4000 K. The fact that such region is located around a height of 200 km in standard semi-empirical models, where the kinetic temperature is about 5000 K, leads us to suggest that the most likely Q/I profile produced by the sun in the lithium doublet should be slightly asymmetric and dominated by the ^{7}Li I peak.

Subject headings: Polarization - Scattering - Sun: atmosphere

1. INTRODUCTION

One of the interesting peculiarities of the linearly-polarized spectrum observed by Stenflo & Keller (1997) in quiet regions close to the solar limb is that a variety of spectral lines from minority species, which produce almost negligible absorption features in the Fraunhofer spectrum, nonetheless stand up with significant contrast in fractional linear polarization (i.e., in the $Q(\lambda)/I(\lambda)$ spectrum)[1]. For example, molecules make a significant contribution to the structural richness of this so-called Second Solar Spectrum, and it is of interest to note that their magnetic sensitivity through the Hanle effect has facilitated the exploration of the sun's hidden magnetism (see the detailed review by Trujillo Bueno et al. 2006, and more references therein). Spectral lines from rare earths, such as those from ionized cerium, are also of interest for obtaining information on unresolved, tangled magnetic fields in the "quiet" solar atmosphere (see Manso Sainz et al. 2006). The main aim of this paper is to investigate the physical origin and the diagnostic potential of what is probably the weakest Q/I spectral feature produced by a minority species in the whole Second Solar Spectrum: that observed by Stenflo et al. (2000) in the Li I resonance doublet at 6708 Å (see Figure 1). Although it is generally accepted that the Second Solar Spectrum is due to radiatively induced population imbalances and quantum coherences in the atoms and molecules of the solar atmosphere, and several interesting spectral lines have been successfully modeled (e.g., Manso Sainz & Trujillo Bueno 2003), much remains to be done to fully understand the Q/I profiles observed in many other spectral lines.

As seen in Figure 1, the line center value of the observed Q/I profile published by Stenflo et al. (2000) is only 2×10^{-4}, and its detection required to sacrifice completely the spatio-temporal resolution in order to be able to push down the *rms* noise to below the 10^{-5} level. The FWHM of the observed Q/I profile is about 190 mÅ. The most peculiar feature of the observed signal is its three-peak structure, which bears a qualitative resemblance to the triple peak structure of the Q/I profile observed in the Na I D_2 line. Like the sodium doublet, the Li I one at 6708 Å results from a D_2 type transition ($J_u = 3/2$ and $J_\ell = 1/2$) and a D_1 type transition ($J_u = 1/2$ and $J_\ell = 1/2$), with the difference that lithium has two isotopes: ^{7}Li (with nuclear spin $I = 3/2$ and a relative meteoritic abundance of 92.41%) and ^{6}Li (with $I = 1$ and a relative meteoritic abundance of 7.59%). The fact that quantum interferences between the $J_u = 3/2$ and $J_u = 1/2$ levels are indeed important for understanding the Q/I pattern observed at wavelengths around the sodium D_2 and D_1 lines (Stenflo & Keller 1997; Landi Degl'Innocenti 1998) led Stenflo et al. (2000) to argue that the Q/I feature shown in Figure 1 must be seriously influenced by a quantum mechanical superposition of the scattering transitions in the D_2 and D_1 lines of lithium.

An accurate measurement of the very weak linear polarization signal of the Li I doublet at 6708 Å is so difficult that we believe that it is very important to investigate care-

[1] Note that the first Stokes parameter, $I(\lambda)$, is the specific intensity at a given wavelength, while Stokes $Q(\lambda)$ represents here the intensity difference between linear polarization parallel and perpendicular to the closest solar limb.

TABLE 1
PHYSICAL PROPERTIES OF THE TWO STABLE ISOTOPES OF LITHIUM

Isotope	Abund.	I	Isotope Shifts (MHz)[a]		HFS Constants (MHz)		
	(%)[b]		D_1	D_2	$^2S_{1/2}$	$^2P_{1/2}$	$^2P_{3/2}$
					$\mathcal{A}$	$\mathcal{A}$	$\mathcal{A}$
							$\mathcal{B}$
^{6}Li	7.59	1	-10533.13[c]	-10534.93[c]	152.1368393[d]	17.375[e]	-1.155[e]
							-0.010[e]
^{7}Li	92.41	3/2	reference isotope		401.7520433[d]	45.914[f]	-3.055[f]
							-0.221[f]

[a]A positive isotope shift means that the line is shifted to higher frequencies with respect to the reference isotope. [b]Ralchenko et al. (2008); [c]Scherf et al. (1996); [d]Beckmann et al. (1974); [e]Orth et al. (1974); [f]Orth et al. (1975).

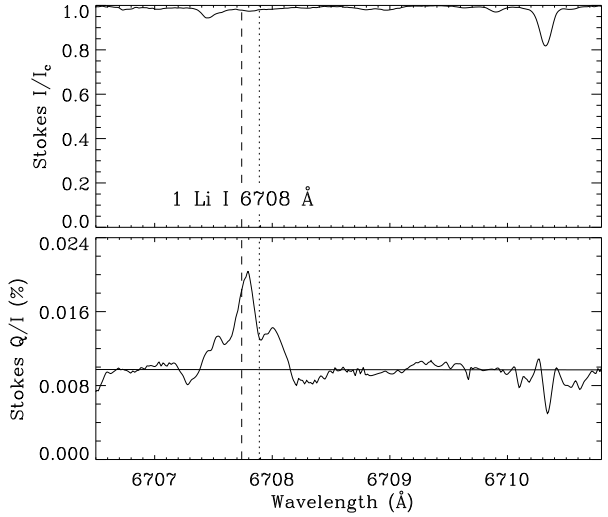

FIG. 1.— Intensity spectrum (upper panel) and fractional linear polarization (lower panel) of the Li I 6708 Å doublet, as observed by Stenflo et al. (2000). The wavelength positions of the two components of this doublet (which are of the D_2 and D_1 type), due to the most abundant lithium isotope (^{7}Li), are indicated by the dashed and dotted lines, respectively. The recording was made on 1996 September 8, near the south polar limb. From Stenflo et al. (2000).

fully whether or not the Q/I profile observed by Stenflo et al. (2000) can be confirmed by theory. We think that this can be achieved with a particularly high level of confidence for this lithium doublet, because its extreme weakness in the intensity spectrum suggests that radiative transfer effects play no significant role on the *shape* of the Q/I profile. Indeed, the anisotropic radiation pumping is basically that due to the solar continuum radiation. Moreover, since the incident radiation field is practically flat across the lithium doublet, we can rigorously apply the complete redistribution theory of spectral line polarization (see the monograph by Landi Degl'Innocenti & Landolfi 2004, hereafter referred to as LL04), either neglecting or accounting for quantum interferences between the hyperfine structure (HFS) F-levels pertaining to the $J_u = 3/2$ and $J_u = 1/2$ levels.

As we shall see, the application of the above-mentioned quantum theory of spectral line polarization leads to the conclusion that only two peaks can be expected for the Q/I profile of the Li I resonance doublet at 6708 Å. Interestingly, we find that the strongest peak at 6707.75 Å is caused by the D_2 line of ^{7}Li I, while the weakest one at about 6707.9 Å is due to the D_2 line of ^{6}Li I. Since in the sun the line opacity of this lithium doublet is negligible with respect to that of the continuum, contrary to the case of strong lines like Na I D_1 and D_2, or Ca II H and K, these lithium lines neither show extended wings in the intensity spectrum nor in the Q/I spectrum, the continuum level being rapidly reached as one moves away from line center. This explains why quantum interferences between HFS F-levels pertaining to different J-levels, whose signatures are negligible in the line core but become dominant in the wings, are found to play no significant role on the emergent Q/I profile of this lithum doublet. Moreover, we find that such two peaks in the theoretical Q/I profile stand up clearly only when the kinetic temperature of the thin atmospheric region that produces the emergent Q/I profile is lower than 4000 K. In order to be able to reproduce the width of the observed Q/I profile without accounting for non-thermal broadening we need at least 6000 K, but for $T > 5000$ K the predicted Q/I profile is slightly asymmetric (i.e., with a more extended red wing) and only shows the dominant peak due to ^{7}Li I.

The outline of the paper is the following. In Section 2, we present the atomic model and the structure of the hyperfine multiplets, both of ^{6}Li I and of ^{7}Li I. In the same section, we briefly present the density matrix formalism which we have adopted in order to describe the atomic polarization induced in the various levels by anisotropic radiation pumping processes. The optically thin slab model considered in this investigation, and the relevant equations describing the polarization of the emergent radiation are discussed in Section 3. In Section 4, the resulting theoretical Q/I profile is shown, and the physical origin of its spectral features is investigated. Section 4.1 is dedicated to a discussion of the role of quantum interferences between the upper J-levels of the D_1 and D_2 lines. Finally, the sensitivity of the resulting profile to the isotopic abundances and to microturbulent magnetic fields is discussed in Section 5. Section 6 collects our conclusions with an outlook to future research.

2. THE ATOMIC MODEL

We adopt a three-level model of Li I consisting in the ground level ($2s\ ^2S_{1/2}$), the upper level of the D_1 line ($2p\ ^2P_{1/2}$), and the upper level of the D_2 line ($2p\ ^2P_{3/2}$). The energies of the fine structure levels are taken from Ralchenko et al. (2008). In order to take into account the isotopic effect, we correct the energies of the $^2P_{1/2}$ and of the $^2P_{3/2}$ levels of ^{6}Li I using the values of the isotopic shifts in the D_1 and D_2 lines

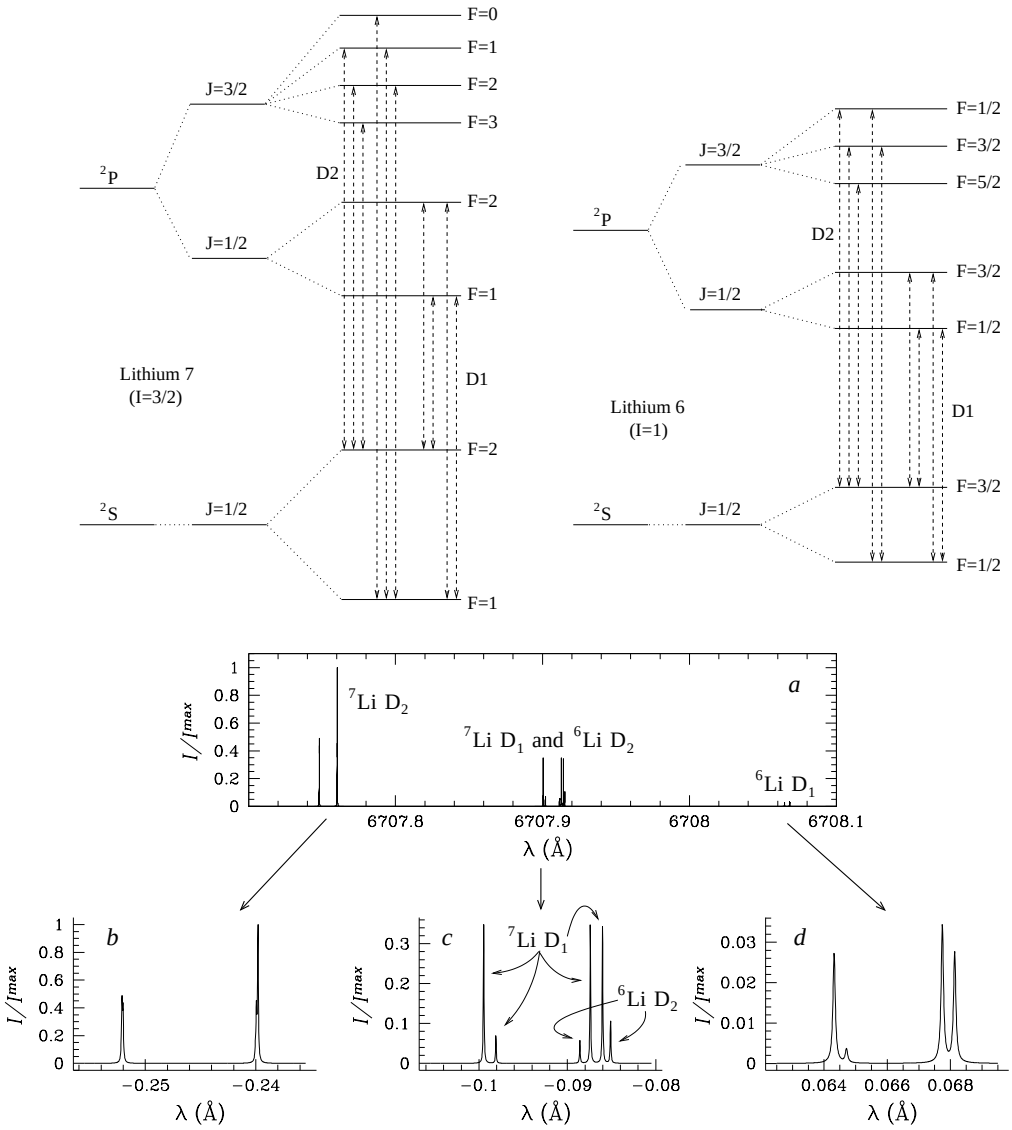

FIG. 2.— Grotrian diagram showing the terms, the fine structure, and the hyperfine structure levels considered in our atomic models for the ^{6}Li and ^{7}Li isotopes (splittings are not drawn to scale). On the Grotrian diagrams the HFS components of the D_1 and D_2 lines of both isotopes are drawn. Panel *a* shows the laboratory positions and relative intensities of all the HFS components, as obtained taking into account the meteoritic relative abundance of the two isotopes. Panels *b*, *c* and *d* show in more detail the HFS components of the ^{7}Li I D_2 line (*b*), the HFS components of the ^{7}Li I D_1 line together with those of the ^{6}Li I D_2 line (*c*), and the HFS components of the ^{6}Li I D_1 line (*d*). Note that the scale of the I/I^{max} graph is different in the various panels. The zero of the wavelength scale in panels *b*, *c* and *d* is taken at 6708 Å.

listed in Table 1.

The HFS Hamiltonian, describing the interaction between the nuclear spin and the electronic angular momentum, can be expressed as a series of electric and magnetic multipoles (see, for example, Kopfermann 1958). We calculate the energies of the HFS F-levels using the values of the magnetic dipole and of the electric quadrupole HFS constants (usually indicated with the symbols $\mathcal{A}$ and $\mathcal{B}$, respectively) listed in Table 1. We recall that in the absence of magnetic fields, using Dirac's notation, the energy eigenvectors can be written in the form $|\alpha JIFf>$, where α represents a set of inner quantum numbers (specifying the configuration and, if the atomic system is described by the L-S coupling scheme, the total electronic orbital and spin angular momenta), J is the total electronic angular momentum quantum number, while F and f are the quantum numbers associated with the total angular momentum operator (electronic plus nuclear: **F=J+I**), and with its projection along the quantization axis, respectively. The Grotrian diagrams showing the various HFS F-levels of the two isotopes, and the HFS components of the D_1 and D_2 lines are shown in the upper panel of Figure 2. In the lower panels of Figure 2 the laboratory positions of the various HFS components are shown. Since the isotopic shifts are of the same order of magnitude as the frequency separation between the two D-lines, the D_1 line of ^{7}Li I falls almost at the same wavelength as the D_2 line of ^{6}Li I (see panels *a* and *c* of Figure 2). We observe that in both isotopes the ground level splits into two HFS F-levels. The splitting between these two levels is much larger than that among the HFS F-levels pertaining to the upper levels. As a consequence, the HFS components both of the D_1 and of the D_2 lines can be gathered into two groups. Note also that it is not possible to resolve, even in the laboratory spectra, all the HFS components of the D_2 line, since their frequency separation is smaller than the natural width

TABLE 2
WAVELENGTHS (IN AIR) AND EINSTEIN COEFFICIENTS OF THE LINES CONSIDERED; MEAN NUMBER OF PHOTONS AND ANISOTROPY FACTOR OF THE PHOTOSPHERIC CONTINUUM AT THE WAVELENGTHS OF THE SAME LINES.

Line	λ (Å)	$A(s^{-1})$	$\bar{n}_\nu$	w_ν
D_1	6707.91	3.72×10^7	0.0115	0.0992
D_2	6707.76	3.72×10^7	0.0115	0.0992

(compare the magnetic dipole HFS constant of the D_2 upper level with the Einstein coefficient for spontaneous emission in this line, quoted in Table 2).

We describe the excitation state of the Li I levels by means of the density matrix formalism, a robust theoretical framework very suitable for treating the atomic polarization (population unbalances, and quantum interferences among the magnetic sublevels) that can be induced, for instance, by an anisotropic incident radiation field. In principle, to have a complete description of the atomic polarization, one has to take into account all the quantum interferences (or coherences) of the form

$$< \alpha JIF\, f\, |\hat{\rho}|\, \alpha J'IF'\, f' > \ , \qquad (1)$$

where $\hat{\rho}$ is the density operator. In this investigation we, first, restricted to the J-diagonal density matrix elements

$$< \alpha JIF\, f\, |\hat{\rho}|\, \alpha JIF'\, f' > \ , \qquad (2)$$

or, in other words, we neglected coherences between different J-levels. According to LL04, the resulting model atom is referred to as *multi-level atom with HFS*. The statistical equilibrium equations (SEE), and the radiative transfer coefficients for a multi-level atom with HFS can be found in LL04. More general calculations, that we carried out including the interferences between the upper HFS levels of the D_1 and D_2 lines, showed that the previous approximation is fully justified for the investigation of this lithium doublet. Indeed, as it will be shown in Section 4.1, the theoretical Q/I profiles obtained through the solution of these more general equations cannot be distinguished from those shown in this paper, which, as mentioned above, neglect quantum interferences between different J-levels. This is due to the weakness of the lithium doublet which does not allow for the formation of extended wings where such quantum interferences would produce their main signatures.

3. THE OPTICALLY THIN SLAB MODEL

In order to emphasize the atomic aspects involved in the problem, avoiding complications due to radiative transfer effects, we consider a horizontal, optically thin slab of Li I ions. We assume the slab to be illuminated from below by the observed photospheric continuum radiation field, that we suppose to be unpolarized and cylindrically symmetric about the local vertical. Under these assumptions, taking a reference system with the z-axis (the quantization axis) directed along the vertical, only two components of the radiation field tensor, through which we describe the incident continuum radiation, are non-vanishing:

$$J^0_0(\nu)=\oint \frac{d\Omega}{4\pi} I(\nu,\mu) \quad \text{and} \quad J^2_0(\nu)=\oint \frac{d\Omega}{4\pi} \frac{1}{2\sqrt{2}}(3\mu^2-1) I(\nu,\mu) \ , \qquad (3)$$

where μ is the cosine of the heliocentric angle. The former quantity is the mean intensity of the incident radiation field (averaged over all directions), the second one quantifies its degree of anisotropy (unbalance between vertical and horizontal illumination). Mean intensity and anisotropy degree of the radiation field can also be expressed in terms of two non-dimensional quantities: the average number of photons per mode, $\bar{n}$, and the so-called anisotropy factor, w (which varies between $w=-1/2$, for the case of horizontal illumination by an unpolarized radiation field without azimuthal dependence, and $w=1$ for vertical unpolarized illumination). Such quantities are related to J^0_0 and J^2_0 by the equations

$$\bar{n}(\nu) = \frac{c^2}{2h\nu^3} J^0_0(\nu) \ , \quad w(\nu) = \sqrt{2}\frac{J^2_0(\nu)}{J^0_0(\nu)} \ . \qquad (4)$$

We calculate the values of $\bar{n}(\nu)$ and $w(\nu)$ of the photospheric continuum at the frequencies of the Li I D-lines, following Section 12.3 of LL04 taking $h=0$, and using the values of the disk-center intensities and of the limb-darkening coefficients given by Pierce (2000). The values obtained are listed in Table 2. Once the SEE have been written down and solved numerically, we can calculate the radiative transfer coefficients. We consider the radiation scattered by the slab at 90°, and we take the reference direction for positive Q parallel to the slab. For the case of a tangential observation, in a weakly polarizing atmosphere ($\varepsilon_I \gg \varepsilon_Q, \varepsilon_U, \varepsilon_V; \eta_I \gg \eta_Q, \eta_U, \eta_V, \rho_Q, \rho_U, \rho_V$), the polarization of the emergent radiation is given by (see Trujillo Bueno 2003)

$$\frac{X(\nu,\mathbf{\Omega})}{I(\nu,\mathbf{\Omega})} \approx \frac{\varepsilon_X(\nu,\mathbf{\Omega})}{\varepsilon_I(\nu,\mathbf{\Omega})} - \frac{\eta_X(\nu,\mathbf{\Omega})}{\eta_I(\nu,\mathbf{\Omega})} \qquad \text{with } X=Q,U,V \ . \qquad (5)$$

The first term in the right hand side of Eq. (5) represents the contribution to the emergent radiation due to selective emission processes, the second one is caused by dichroism (selective absorption of polarization components).

The way atomic polarization is distributed among the various levels by radiative processes is very similar to the case of the sodium and barium D-lines, investigated by Trujillo Bueno et al. (2002) and by Belluzzi et al. (2007), respectively. We recall in particular that only the upper level of the D_2 line can be directly polarized by the anisotropic incident radiation field. The ground level becomes polarized because of a transfer of atomic polarization via spontaneous emission in the D_2 line, while the D_1 upper level is polarized via radiative absorption in the D_1 line ("repopulation pumping"). Indeed, solving the SEE in the absence of magnetic fields, one finds that the D_2 line upper level is considerably more polarized than both the D_1-line upper level and the ground level. Dichroism therefore can be safely neglected as far as D_2 is concerned, while it is expected to be more important in the D_1 line. However, given that the polarization signal produced by the D_1 line of Li I is expected to be several orders of magnitude smaller than the one produced by the D_2 line, we neglect dichroism also in the D_1 line. We calculate therefore the polarization of the emergent radiation through the simpler equation

$$\frac{X(\nu,\mathbf{\Omega})}{I(\nu,\mathbf{\Omega})} \approx \frac{\varepsilon_X(\nu,\mathbf{\Omega})}{\varepsilon_I(\nu,\mathbf{\Omega})} \ . \qquad (6)$$

The emission coefficients that appear in the previous equation include only line processes: in order to reproduce the observed Q/I profile, we need to add the contribution of the continuum. Assuming such contributions to be constant across

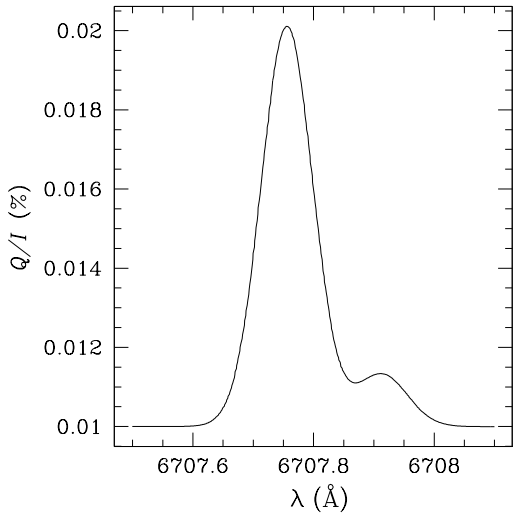

FIG. 3.— Theoretical Q/I profile obtained assuming the following values of the free parameters: $\varepsilon_I^{\rm c} = 200 \times \varepsilon_I^{\rm max}$, $\varepsilon_Q^{\rm c} = 10^{-4} \times \varepsilon_I^{\rm c}$. The profile is obtained for a Doppler width of 60 mÅ, which corrresponds to $T \approx 3000$ K.

the line we have

$$\frac{X(\nu,\mathbf{\Omega})}{I(\nu,\mathbf{\Omega})} \approx \frac{\varepsilon_X^{\ell}(\nu,\mathbf{\Omega}) + \varepsilon_X^{c}}{\varepsilon_I^{\ell}(\nu,\mathbf{\Omega}) + \varepsilon_I^{c}} \quad , \tag{7}$$

where the superscripts "c" and "ℓ" recall that the corresponding quantities refer to continuum and line processes, respectively. The quantities $\varepsilon_X^{\rm c}$ and $\varepsilon_I^{\rm c}$ will be considered as free parameters to be adjusted in order to reproduce the observed polarization profile. The effect of collisions will be neglected throughout this investigation. It should be observed that given the extreme weakness of the absorption features of this lithium doublet in the solar intensity spectrum, the optically thin slab model is expected to be a rather good approximation for the modelling of these lines.

4. THEORETICAL LINEAR POLARIZATION PROFILE OF THE EMERGENT RADIATION

Applying Eq. (7), and assuming the following values of the free parameters $\varepsilon_I^{\rm c} = 200 \times \varepsilon_I^{\rm max}$, where $\varepsilon_I^{\rm max}$ is the maximum value of ε_I^{ℓ} in the wavelength range considered, $\varepsilon_Q^{\rm c} = 10^{-4} \times \varepsilon_I^{\rm c}$, and a Doppler width of 60 mÅ, we obtain the two-peak linear polarization profile shown in Figure 3. As can be observed in the left panel of Figure 4, modifying the continuum contribution to the intensity we modify the amplitude of the two peaks, without changing the shape of the profile.

The value that we assumed for the continuum contribution ($\varepsilon_I^{\rm c} = 200 \times \varepsilon_I^{\rm max}$) appears to be a good choice, given the weakness of the line, and that it allows the peak falling at shorter wavelengths (hereafter referred to as the "blue peak") to reach the same amplitude (0.02%) as the central peak of the Q/I profile observed by Stenflo et al. (2000) (see Figure 1). The value of $\varepsilon_Q^{\rm c}$ has been adjusted in order to obtain in the far wings the same continuum polarization level as in the observation (0.01%).

Particularly interesting is the sensitivity of the theoretical Q/I profile to the value of the Doppler width. The profile shown in Figure 3 has been obtained assuming a Doppler width of 60 mÅ, which corresponds, neglecting microturbulent velocities, to a temperature of 3000 K. For the sake of simplicity, we consider the same Doppler width for the two isotopes, despite their mass difference ($\approx$ 14%)[2]. Profiles obtained assuming different values of the Doppler width are plotted in the right panel of Figure 4. Interestingly, we observe that the two-peak structure gradually disappears as the Doppler width is increased: the observation of a two-peak structure could thus provide precise information concerning the thermal properties of the thin atmospheric region where this weak lithium doublet is formed.

In the left panel of Figure 5, the same Q/I profile as in Figure 3 is plotted together with the profiles expected in the hypothetical cases where only ^{6}Li (short-dashed line) or only ^{7}Li (long-dashed line) were present. The polarization peak that is obtained when a single isotope is considered (either ^{6}Li or ^{7}Li) is, in both cases, due to the corresponding D_2 line. Indeed, the polarization signals produced by the D_1 lines, both of ^{6}Li I and of ^{7}Li I, are several orders of magnitude smaller, and cannot be appreciated on this plot. It is then clear that the physical origin of the two-peak structure of the Q/I profile that we have obtained within our modelling assumption lies in the isotopic shift between the two lithium isotopes: the two peaks are nothing else but the signals produced by the D_2 lines of ^{7}Li I (blue peak) and of ^{6}Li I (red peak), which fall at different wavelengths because of the isotopic shift, and which are weighted by the isotopic abundances.

It is also interesting to observe that the signals due to the D_2 lines of the two isotopes, as found in the hypothetical cases where only ^{6}Li or only ^{7}Li were present, do not have the same amplitude (see the left panel of Figure 5). This is due to the fact the two isotopes have different HFS (in particular different nuclear spin quantum numbers, and different HFS constants, producing different splittings among the various F-levels, so that ^{6}Li is less depolarized by HFS than ^{7}Li). As a consequence, the relative amplitude of the two peaks that we have found in the resulting Q/I profile does not reflect only the different abundances of the two lithium isotopes, but also their different HFS. Therefore, the presence of HFS in the two isotopes has to be taken into account in order to obtain the correct relative amplitude between the two peaks. This is clearly shown in the right panel of Figure 5, where the profiles obtained including (solid line) and neglecting (dashed line) HFS are plotted.

4.1. *The role of coherences between the upper J-levels of the Li I D_1 and D_2 lines*

Although the D_1 and D_2 lines (both of ^{6}Li I and ^{7}Li I) are very close to each other, so that quantum interferences between the upper levels of the corresponding transitions are not negligible, it is important to point out that, because of the weakness of these lines, the continuum level is rapidly reached both in the intensity spectrum, and in the Q/I spectrum, and the spectral signatures of such coherences are completely lost. This can be easily appreciated in Figure 6, where the theoretical Q/I profiles, obtained both without (upper panel) and with (lower panel) continuum, are plotted according to three different approximations: *a*) taking into account HFS, but neglecting interferences between pairs of HFS magnetic sublevels pertaining to different J-levels (solid line), *b*) neglecting HFS, but taking into account interferences be-

[2] Note that calculations made taking into account the mass difference between the two isotopes have not shown any appreciable modification of the results.

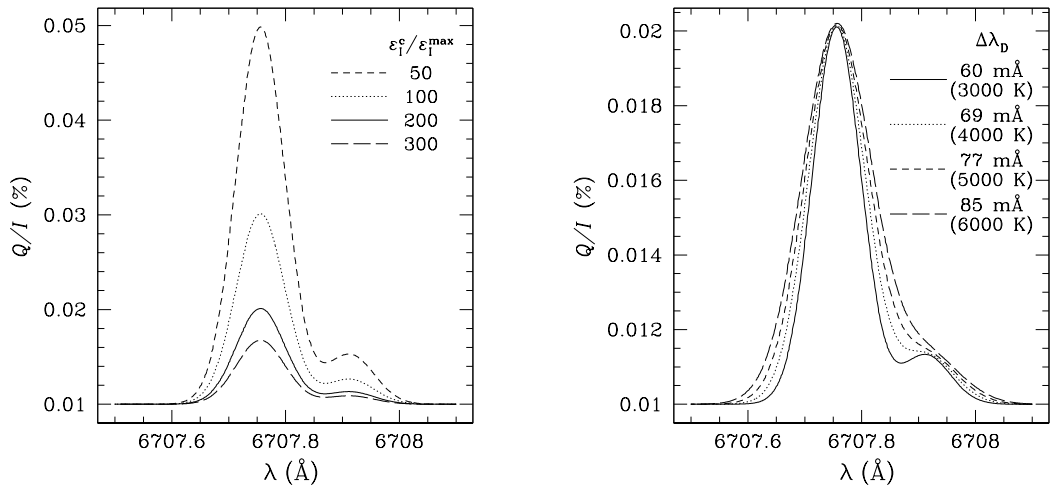

FIG. 4.— Left panel: theoretical Q/I profiles obtained for different values of the continuum (ε_I^c). The solid-line profile is the same as in Figure 3. Right panel: theoretical Q/I profiles obtained for different values of the Doppler width ($\Delta\lambda_D$). The solid-line profile is the same as in Figure 3.

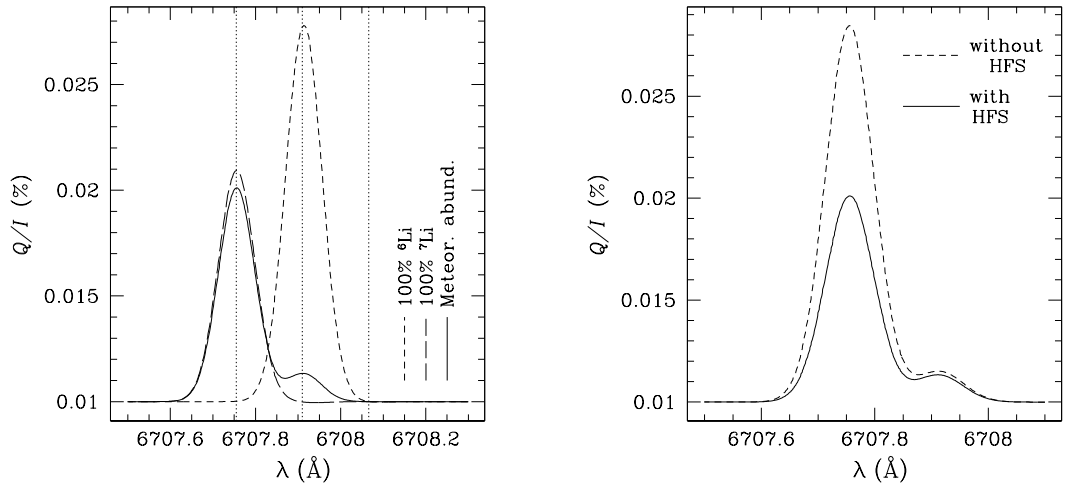

FIG. 5.— Left panel: theoretical Q/I profiles obtained (*a*) considering both isotopes weighted by their meteoritic abundances (solid line), (*b*) assuming that only ^{6}Li (100% in abundance) is present (short-dashed line), (*c*) assuming that only ^{7}Li (100% in abundance) is present (long-dashed line). The vertical dotted lines show the wavelength positions of the HFS components of the ^{7}Li I D_2 line (first line going from shorter to longer wavelengths), of the ^{7}Li I D_1 line together with the ^{6}Li I D_2 line (middle line), and of the ^{6}Li I D_2 line (last line). The solid-line profile is the same as in Figure 3. Right panel: theoretical Q/I profiles obtained considering both isotopes, weighted by their meteoritic abundances, taking into account (solid line) and neglecting (dashed line) HFS. The solid-line profile is the same as in Figure 3. All profiles have been obtained for a Doppler width of 60 mÅ.

tween pairs of magnetic sublevels pertaining to different J-levels (dotted line), and *c*) taking into account HFS, and taking also into account interferences between pairs of HFS magnetic sublevels pertaining to different J-levels (dashed line). The first approximation is the one that has been applied in this paper (see Section 2). A detailed description of the other approximations, usually referred to as *multi-term atom* and *multi-term atom with HFS* can be found in LL04, and in Casini & Manso Sainz (2005), respectively.

We start considering the results obtained without continuum (upper panel). As expected, close to line center there is no appreciable difference between the profile obtained including the interferences between the upper levels of the D_1 and D_2 lines (dashed-line profile) and the one obtained neglecting such interferences (solid-line profile). Actually, we recall that such interferences play an important role in the wings of the line, being negligible close to the line core. At line center, on the other hand, there is an appreciable difference between the profiles obtained taking into account (solid- and dashed-line profiles) and neglecting (dotted-line profile) HFS. In the far wings, on the contrary, as can be observed by comparing the dashed- and the dotted-line profiles, there is no difference between the results obtained by taking into account or neglecting HFS (as known, the effect of HFS vanishes in the far wings of the line)[3]. At these wavelengths, on the other hand, the interferences between different J-levels become important, and their effect can be easily appreciated. In particular, we observe that the asymptotic value reached by the profiles obtained taking into account such interferences (dashed- and dotted-line profiles) is much higher than the one reached by the profile calculated neglecting these interferences (solid-line profile).

[3] Note that this is strictly true only if the lower level is not polarized, or if it carries an amount of atomic polarization much smaller than that of the upper level, as in the lines under investigation.

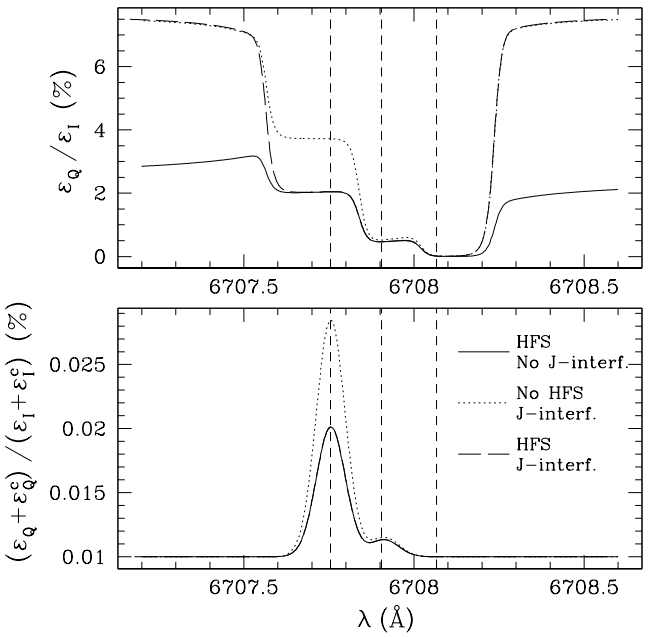

FIG. 6.— Upper panel: theoretical fractional polarization profiles obtained in the absence of continuum according to three different approximations (see the text). The quantities $\bar{n}$, w, and $\Delta\lambda_D$ have the same values as in Figure 3. The vertical dashed lines show the wavelength positions (going from the blue to the red) of ^{7}Li I D_2, of ^{7}Li I D_1 and ^{6}Li I D_2 (blended), and of ^{6}Li I D_1. Lower panel: same as the upper panel, but including the contribution of the continuum. The quantities ε_I^c and ε_Q^c have the same values as in Figure 3. The profile plotted with solid line is the same as in Figure 3.

However, if the continuum contributions to Stokes I and Q are included, so that a two-peak profile with the same amplitude as the observed one is obtained, the polarization in the wings of the line is rapidly decreased to the continuum level, so that the profile obtained by taking into account the interferences between different J-levels cannot be distinguished from the one obtained neglecting such interferences (see the lower panel of Figure 6, where the solid and dashed lines superimpose). The only difference that can still be noticed is at line center, between the profiles obtained by including and neglecting HFS (as already shown in the left panel of Figure 5). We point out that the depolarization of the Q/I profile in the wings of the line, which has completely hidden the signatures of the interferences between the different J-levels, is particularly strong in these lines since a significant continuum contribution ($\varepsilon_I^c = 200 \times \varepsilon_I^{\max}$) is needed in order to reproduce the amplitude ($\approx 10^{-4}$) of the observed Q/I profile. Nevertheless, as already pointed out, this is a rather realistic value, given the extreme weakness of this lithium doublet[4]. In conclusion, as anticipated in Section 2, interferences between the upper levels of the D_1 and D_2 lines, though present, can be safely neglected in the modelling of these lines.

5. SENSITIVITY TO THE ISOTOPIC ABUNDANCE AND TO A MICROTURBULENT MAGNETIC FIELD

In the left panel of Figure 7 the profiles obtained changing the relative abundance of the two isotopes are plotted. We observe that as the ^{6}Li abundance is increased, the amplitude of the blue peak decreases, while the amplitude of the red one increases. This behavior suggests the possibility of using the relative amplitude of the two peaks to estimate the abundance ratio of the two lithium isotopes in the quiet solar atmosphere. Note that the two peaks have a slightly different sensitivity to the relative isotopic abundance. This is probably due to the fact that the blue peak is only caused by the ^{7}Li I D_2 line, whereas the red peak, though dominated by the ^{6}Li I D_2 line, is also affected by the ^{7}Li I D_1 line. Obviously the amplitude of the two peaks of this Q/I profile is not sensitive only to the isotopic abundance, but also to collisions (here neglected), and to the presence of a magnetic field. As it can be observed in the right panel of Figure 7, in the presence of a unimodal microturbulent and isotropic magnetic field the amplitude of the two peaks is reduced because of the Hanle effect. Note that the two peaks have a slightly different magnetic sensitivity (for example, the relative depolarization that takes place going from 1 to 2 G is larger in the red peak). This is due to the fact that the two isotopes have different nuclear spin quantum numbers and different HFS splittings. The saturation regime is reached for magnetic fields of about 50 G. In conclusion, a correct estimate of the lithium isotopic abundance from the relative amplitude of the two peaks of the Q/I profile would require an independent determination of the magnetic field strength present in the regions of the solar atmosphere that produce the observed scattering polarization. Likewise, for a given approximate value of the lithium isotopic abundance the two peaks of the Q/I profile of the lithium doublet can be used to obtain information on the strength of unresolved, hidden magnetic fields in the "quiet" sun. The problem is that it is unlikely that such two peaks can indeed be observed (see below).

6. CONCLUDING COMMENTS

The application of the quantum theory of spectral line polarization leads to the conclusion that only two peaks can be expected for the Q/I profile of the Li I resonance doublet at 6708 Å. Interestingly, we find that the strongest peak at about 6707.75 Å is caused by the D_2 line of ^{7}Li I, while the weakest one at about 6707.9 Å is due to the D_2 line of ^{6}Li I. Since for the lithium doublet in the sun the line opacity is negligible with respect to that of the continuum, we find that quantum interferences between the HFS levels pertaining to different J-levels play no significant role on the emergent Q/I profile. Moreover, we have showed that such two peaks in the theoretical Q/I profile stand up clearly only when the kinetic temperature of the thin atmospheric region that produces the main contribution to the emergent Q/I profile is sufficiently low (e.g., sensibly lower than 4000 K). In order to be able to reproduce the width of the observed Q/I profile, without accounting for non-thermal broadening, we need at least 6000 K, but for this kinetic temperature the predicted Q/I profile is slightly asymmetric (i.e., with a more extended red wing) and shows only the dominant peak due to ^{7}Li I. In this respect, it is of interest to note that the height in standard semi-empirical models of the solar atmosphere where the continuum optical depth at the wavelength of the lithium doublet is unity for a line-of-sight with $\mu = 0.1$ is slightly below 200 km (see Figure 6 of Trujillo Bueno & Shchukina 2009), where the kinetic temperature is about 5000 K. For this reason, we believe that the most likely *shape* of the scattering polarization profile of the lithium doublet that the sun can produce should be similar to the short-dashed line of the right panel of Figure 4.

If that is the case (i.e., if the true Q/I profile of the lithium

[4] Note that also for smaller values of ε_I^c the effects of the interferences between different J-levels turn out to be hidden.

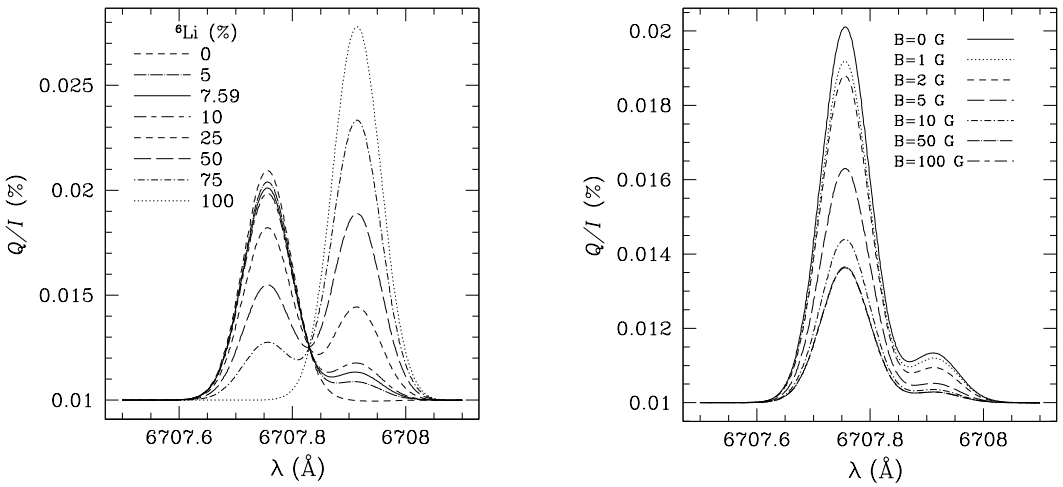

FIG. 7.— Left panel: theoretical Q/I profiles obtained for different isotopic abundances. Right panel: theoretical Q/I profiles obtained in the presence of a microturbulent magnetic field of various intensities, assuming the meteoritic abundances. All the profiles are obtained through Eq. (7), taking the values of the parameters specified in Section 4. The solid-line profile, both in the left and in the right panel, is the same as in Figure 3. All profiles have been obtained for a Doppler width of 60 mÅ.

doublet turns out to have only one peak) then it would not be possible to apply the "peak-ratio technique" illustrated in Figure 7, neither for determining the relative lithium isotopic abundances nor for estimating the strength of an unresolved, hidden magnetic field in the solar photosphere. Nevertheless, the amplitude, FWHM, and asymmetry of the observed Q/I profile could still be used for such a purpose through radiative transfer simulations in a realistic model of the thermal and density structure of the quiet solar photosphere. For example, if the relative lithium isotopic abundance is known beforehand, the discrepancy between the Q/I profile calculated in a three-dimensional hydrodynamical model of the solar photosphere and the observed profile could be interpreted in terms of an unresolved magnetic field, assuming that the depolarizing impact of elastic collisions is properly taken into account in the calculations. Since the relevant pumping radiation field here is that of the continuum radiation, whose anisotropy factor is significantly larger above the granule cell centers than above the intergranular lanes (see Figure 2 of Trujillo Bueno et al. 2004), the observed Q/I profile of the lithium doublet (which lacks spatio-temporal resolution) must be significantly biased towards the granule cell centers. Therefore, we anticipate that the inferred magnetic field strength would be more representative of the magnetization of the granular plasma.

Obviously, new and very careful observations of this extremely weak polarization signal are urgently needed. In this respect, it is of interest to mention that our colleagues from the Istituto Ricerche Solari Locarno (IRSOL), Dr. M. Bianda and Dr. R. Ramelli, have already initiated such an observational program with the Zürich Imaging Polarimeter (ZIMPOL) attached to the Gregory Coudé Telescope of IRSOL. Although some of the Q/I profiles they have been able to measure with such an excellent facility for high-sensitivity spectropolarimetry seem to show a one-peak profile, many more observations are needed in order to fully clarify what type of Q/I profiles the sun is actually producing in the lithium doublet and in order to use them for diagnostic purposes.

The authors wish to thank Dr. Roberto Casini for providing a code that has been very useful for the computations contained in Section 4.1. One of us, ELD, wishes to express his gratitude to the Instituto de Astrofísica de Canarias (IAC) for finantial support that facilitated a sabatical stay at the IAC during 2009. Financial support by the Spanish Ministry of Science through project AYA2007-63881 is also gratefully acknowledged.

REFERENCES

Beckmann, A., Böklen, K.D., & Elke, D. 1974, Z. Phys., 270, 173
Belluzzi, L., Trujillo Bueno, J., & Landi Degl'Innocenti, E. 2007, ApJ, 666, 588
Casini, R., & Manso Sainz, R. 2005, ApJ, 624, 1025
Kopfermann, H. 1958, "Nuclear Moments" (New York: Academic Press)
Landi Degl'Innocenti, E. 1998, Nature, 392, 256
Landi Degl'Innocenti, E., & Landolfi, M. 2004, 'Polarization in Spectral Lines' (Dordrecht: Kluwer) (LL04)
Manso Sainz, R., & Trujillo Bueno, J. 2003, Phys. Rev. Letters, 91, 11, 111102-1
Manso Sainz, R., Landi Degl'Innocenti, E., & Trujillo Bueno, J. 2006, A&A, 447, 1125
Orth, H., Veit, R., Ackermann, H., & Otten, E. W. 1974, in Abstracts of Contributed Papers to the 4th International Conference on Atomic Physics, ed. J. Kowalski & H.G. Weber (Heidelberg: Heidelberg University Press), 93
Orth, H., Ackermann, H., & Otten, E.W. 1975, Z. Phys. A, 273, 221
Pierce, K. 2000, in Allen's Astrophysical Quantities, ed. A. N. Cox (4th ed.; New York: Springer), 355
Ralchenko, Yu., Kramida, A.E., Reader, J., & NIST ASD Team 2008, NIST Atomic Spectra Database (version 3.1.4) (Gaithersburg, MD.: NIST) [Online]
Scherf, W., Khait, O., Jäger, H., & Windholz, H. 1996, Z. Phys. D: At., Mol. Clusters, 36, 31
Stenflo, J.O., & Keller, C.U. 1997, A&A, 321, 927
Stenflo, J.O., Keller, C.U., & Gandorfer, A. 2000, A&A, 355, 789
Trujillo Bueno, J. 2003, New Diagnostic Windows on the Weak Magnetism of the Solar Atmosphere, in Solar Polarization 3, ed. J. Trujillo Bueno & J. Sánchez Almeida, ASP Conf. Ser. 307, 407
Trujillo Bueno, J., & Shchukina, N. 2009, ApJ, 694, 1364
Trujillo Bueno, J., Casini, R., Landolfi, M., & Landi Degl'Innocenti, E. 2002, ApJ, 566, L53
Trujillo Bueno, J., Shchukina, N., & Asensio Ramos, A. 2004, Nature, 430, 326

Trujillo Bueno, J., Asensio Ramos, A., & Shchukina, N. 2006, The Hanle Effect in Atomic and Molecular Lines: A New Look at the Sun's Hidden Magnetism in Solar Polarization 4, ed. R. Casini, & W. Lites, ASP Conf. Ser. 358, 269